

# Type I collagen-chitosan films crosslinked chemically with N-(3-dimethylaminopropyl)-N'-ethylcarbodiimide hydrochloride for guided bone regeneration: A comparative study

J.L. Hidalgo-Vicelis<sup>a\*</sup>, M.A. Alvarez-Perez<sup>b</sup>, S.P. Miranda-Castro<sup>c\*</sup>, M.C. Piña-Barba<sup>a\*</sup>

<sup>a</sup>Laboratorio de Biomateriales, Instituto de Investigaciones en Materiales, Universidad Nacional Autónoma de México, Circuito Exterior s/n, Coyoacán, Ciudad de México, 04510, México

<sup>b</sup>Laboratorio de Bioingeniería de Tejidos, Facultad de Odontología, Universidad Nacional Autónoma de México, Circuito Exterior s/n, Coyoacán, Ciudad de México, 04510, México

<sup>c</sup>Laboratorio de Biotecnología, Facultad de Estudios Superiores Cuautitlán, Universidad Nacional Autónoma de México, Avenida Primero de Mayo s/n, Cuautitlán Izcalli, Estado de México, 54700, México

\*Corresponding autor

## Abstract

In this work, type I collagen-chitosan films were crosslinked chemically with N-(3-dimethylaminopropyl)-N'-ethylcarbodiimide hydrochloride (EDC) in order to improve their physicochemical properties and be used in guided bone regeneration. The films were prepared at different proportions of type I collagen-chitosan by the solvent evaporation technique and crosslinked with EDC. The physicochemical characterization showed that the crosslinked films are more resistant to dehydration, tensile strength and enzymatic digestion. The biological assays using human fetal osteoblasts indicated that the crosslinked films are not cytotoxic. Therefore, the chemical crosslinking with EDC improves the physicochemical properties of the films without affecting to their biocompatibility, indicating that this type of films is a better option for its use in guided bone regeneration.

**Keywords:** Type I collagen; chitosan; N-(3-dimethylaminopropyl)-N'-ethylcarbodiimide hydrochloride; guided bone regeneration.

## 1. Introduction

Bone loss is a very common problem in the area of dental implantology. When a tooth is lost, a reabsorption of the alveolar bone occurs, that in some cases makes it difficult or impossible to place implants [1]. In order to solve these difficulties, the bone tissue augmentation technique known as "guided bone regeneration" has been developed. In this procedure, bone graft is placed in the cavity left by the extraction of a dental piece and a film is surgically inserted onto the filling bone defect to prevent invasion of the cavity by non-osteogenic connective tissue cells, and thus favor the formation of bone tissue [2].

The use of non-resorbable films has demonstrated to be a therapeutic option in the treatment of bone defects, however, the need for a second surgery for their removal and the high frequency of complications associated with this, have produced, in recent years, an increase in the use of resorbable films [1]. The resorbable films can be developed using various natural or synthetic polymers. Currently, natural polymers, such as collagen and chitosan, have been widely used in tissue engineering because they promote the adhesion, growth and differentiation of mesenchymal stem cells [3,4].

Collagen is a fibrous protein secreted by connective tissue cells [5]. It is the main component of the extracellular matrix and the most abundant protein in mammals [6]. Until now, 28 types of collagens are known that differ in their structure, function and distribution in tissues [7]. Type I collagen (Col I) confers strength and toughness to a variety of tissues (e.g., cornea, skin, tendon, dentin and bone) [8]. It is considered one of the most promising biomaterials in tissue engineering due to its biocompatibility and degradability [9].

Chitosan (CS) is a cationic polysaccharide found in the cell walls of some fungi, however, its main production source is the hydrolysis of chitin in an alkaline medium at high temperatures. Chitin is the fundamental material of the exoskeletons of arthropods (e.g., crustaceans, some insects and arachnids) and, after cellulose, it is the most abundant polysaccharide in nature [10]. Chitosan is characterized by its biocompatibility, degradability and its anti-microbial properties [11].

The use of type I collagen and chitosan in tissue engineering is limited by their low thermal and mechanical stability, and high susceptibility to enzymatic degradation [12]. An alternative to improve these physicochemical properties is chemical crosslinking, which promotes the formation of new covalent bonds between the polymer chains. N-(3-dimethylaminopropyl)-N'-ethylcarbodiimide hydrochloride (EDC) has become an attractive crosslinking agent to proteins or chemicals substances that have carboxyl or amino groups because the chemical trace of EDC is not integrated in the polymer chains after crosslinking [13].

There are studies related to collagen-chitosan composites in tissue engineering (e.g., gels, films and sponges). In the case of films made from these natural polymers, the crosslinking with EDC has been studied mainly in the regeneration of cornea [14] and liver [15], however, there are few studies on guided bone regeneration. On the other hand, these studies do not establish a comparative analysis to know the effect of chemical crosslinking, or a limited range of collagen-chitosan proportions is studied.

Therefore, the aim of this work was to establish a comparative study between the physicochemical and biological properties of crosslinked and non-crosslinked films with EDC in a wide range of type I collagen-chitosan proportions, as a proposal for guided bone regeneration strategies.

## **2. Materials and methods**

### *2.1. Extraction and characterization of type I collagen and chitosan*

Col I was extracted from the bovine Achilles tendon (acquired from a TIF slaughterhouse) according to the Miller and Rhodes method [16]. The purity of Col I was analyzed by polyacrylamide gel electrophoresis with sodium dodecylsulfate (SDS-PAGE) [17] and the concentration of the protein was determined by quantifying the hydroxyproline present in the samples as described by Woessner [18].

Chitin was extracted from shrimp exoskeletons and converted to CS according to the Miranda and Lara method [19]. The degree of deacetylation and molecular weight of the polysaccharide were determined by potentiometric titration and capillary viscosimetry, respectively [20,21].

### *2.2. Preparation of Col I and CS films*

The films were produced by the solvent evaporation technique. Col I and CS solutions were prepared separately at a concentration of 0.5% (w/v) in 1% acetic acid (v/v). These solutions were mixed at the following Col I-CS proportions 0:100, 25:75, 50:50, 75:25 and 100:0 (C0, C25, C50, C75 and C100, respectively), deposited in molds and dried at room temperature. Afterward, the films were chemically crosslinked by immersing them in EDC (purity ≥98%, Sigma-Aldrich) under agitation for 21 h, in order to improve their physicochemical properties. Finally, the films were rinsed with deionized water to remove the residues of the crosslinking agent, dried at room temperature and stored in a desiccator until their use. It is important to mention that the obtained films were compared with a commercial film (Membracel®-O, Argentina), which is from native collagen of bovine.

### *2.3. Physicochemical characterization of the films*

The interaction and chemical crosslinking of the polymers (Col I and CS), were analyzed by Fourier transform infrared spectroscopy (FTIR) using an Alpha Platinum equipment from Bruker connected to a diamond cell of attenuated total reflectance (ATR). Each spectrum was an average of 32 scans with a resolution of 4 cm<sup>-1</sup>.

The water absorption capacity by the films was determined by gravimetry doing three replicates of the experiment. The mass was measured to the dry films ( $W_d$ ), then these were immersed in phosphate buffered saline (PBS) and incubated at 37 °C for 24 h, in order to simulate a biological fluid. Finally, the mass was measured ( $W_w$ ), removing excess water over the surface of the films with filter paper. The water absorption percentage by the films was calculated using equation 1.

$$\text{Water absorption (\%)} = \frac{W_w - W_d}{W_d} \cdot 100 \quad (1)$$

The thermal stability of the films was evaluated by thermogravimetric analysis (TGA) and differential scanning calorimetry (DSC) using a TA Instruments Q5000IR and TA Instruments Q2000 equipment, respectively. Both analyzes were carried out with a heating ramp of 5 °C/min in a nitrogen atmosphere.

The mechanical behavior of the films was evaluated by a uniaxial tensile test. The films were hydrated in the same way as in the water absorption experiment and cut according to ASTM-D1708-18. The mechanical response of the wet specimens was evaluated using a CT3™ texture analyzer from Brookfield with a strain rate of 10 mm/min at room temperature. The experiment was carried out in triplicate.

The degradation of the films was evaluated by an enzymatic digestion doing three replicates of the experiment. The mass was measured to the dry films ( $W_i$ ), then these were immersed in 112 000 U/mL lysozyme (95% purity, Sigma)/PBS and incubated at 37 °C at different contact times (0, 3, 6, 12, 24, 72, 120, 168, 336 h). The lysozyme solution was changed every 24 h, in order to maintain the enzymatic activity. At the end of each contact time, the films were removed from the enzyme solution, rinsed with deionized water and dried at 60 °C for 12 h. Finally, the mass was measured ( $W_f$ ) to calculate the mass loss percentage using equation 2.

$$\text{Mass loss (\%)} = \frac{W_i - W_f}{W_f} \cdot 100 \quad (2)$$

The morphology of the films was studied by scanning electron microscopy (SEM, JCM-6000, JEOL) in secondary electron mode with an acceleration voltage of 10 kV at a high vacuum. Before the films were observed, these were washed with PBS, dehydrated in increasing concentrations of ethanol and dried at critical point (CPD, Polaron) of CO<sub>2</sub>, in order to maintain the microstructure of the hydrated state. Finally, they were coated with a thin layer of gold by plasma assisted physical vapor deposition (PAPVD, Polaron) [22].

#### 2.4. Biological characterization of the films

The adhesion, viability and morphology of cells onto the films were evaluated using a human fetal osteoblast cell line (hFOB 1.19 ATCC CRL-11372). The hFOB cells were cultured and expanded in Dulbecco's modified Eagle's medium supplemented with 10% fetal bovine serum, 2 mM L-glutamine and antibiotics (100 IU/mL penicillin, 100 µg/mL streptomycin and 0.3 µg/mL fungizone). Cell cultures were maintained at a temperature of 37 °C, in an atmosphere of 95% air/5% CO<sub>2</sub> and with 100% of humidity. Cultures between the second and sixth passages were used for the assays.

The adhesion of the hFOB cells over the films was evaluated by the crystal violet assay [23]. The osteoblasts were seeded onto the films at a cell density of 1x10<sup>4</sup> cells/mL and cultured for 4 h. Subsequently, the films were washed with PBS to remove the non-adhered cells. The films with the adhered cells were fixed with 4% *p*-formaldehyde for 24 h, washed with PBS, incubated with 0.1% crystal violet (Sigma) for 15 min and rinsed with bidistilled water to remove excess dye. The crystal violet

fixed over the adhered cells was extracted with 200 µL of 1% SDS and the absorbance was measured at 545 nm using a plate reader (Chromate 4300, Awareness Technology, Inc.). The control cultures were the cells seeded onto the culture plate. The obtained absorbance values were converted to percentages of adhered cells considering that the culture plate (Eppendorf) corresponded 100% of adhesion. The experiment was carried out in triplicate.

The viability of the hFOB cells over the films was evaluated using the cell counting kit-8 (CCK-8) doing three replicates of the experiment [24]. The osteoblasts were seeded onto the films at a cell density of  $1 \times 10^4$  cells/mL and cultured for 1, 3, 5, 7 and 14 days. At the end of each culture period, the cells were incubated with 10 µL of the CCK-8 solution (Sigma) for 4 h. Finally, 200 µL of the culture medium were removed, placed in a 96 well plate and the optical density (O.D.) was measured at 450 nm using a plate reader.

The interaction of the hFOB cells over the surface films was studied by SEM. The osteoblasts were seeded onto the films at a cell density of  $1 \times 10^4$  cells/mL and cultured for 24 h. Afterward, the films were washed with PBS to remove the non-adhered cells. The films with the adhered cells were fixed with 4% *p*-formaldehyde and 1% osmium tetroxide for 12 and 2 h, respectively; and washed with PBS at the end of each fixation period [22]. Finally, the samples were dehydrated, dried and coated with gold in the same way as in the study of the films morphology.

### 2.5. Statistical analysis

Data were statistically compared by a one- and two-way analysis of variance (ANOVA) by Tukey, Dunnet and Sidak tests using GraphPad Prism 6.01 statistical software (GraphPad Software Inc., San Diego, CA), considering  $p < 0.05$  as statistically significant.

## 3. Results and discussion

### 3.1. Type I collagen and chitosan

The obtained yield with the method used for the extraction of Col I was 54.6%, which is a higher percentage than the yield reported by Nalinanon *et al.* (41.02%) [25]. The obtained collagen showed the typical structure of Col I (Fig. 1), because the characteristic bands of Col I are present ( $\alpha_1$ : 140.8 kDa,  $\alpha_2$ : 127.6 kDa,  $\beta$ : 240.1 and 256.4 kDa, and  $\gamma$ : 322.7 and 337.2 kDa) [16] and there are no others apart from these.

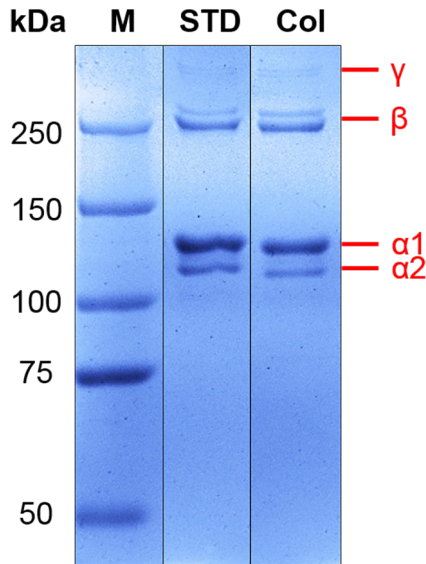


**Fig. 1.** Electrophoretic pattern of type I collagen (Col I). M: molecular weight marker (Precision Plus Protein Standards, Dual Color, Bio-Rad); STD: bovine Col I standard (DSM Nutritional Products Ltd.); and Col: obtained collagen.

In the case of the method used for the extraction of chitin and its conversion to CS, a yield of 24.8% was obtained. The CS presented a high degree of deacetylation of  $96.5 \pm 0.2\%$ , which makes it highly soluble in diluted acids. The average molecular weight of the polymer was  $145.2 \pm 2.0$  kDa, which is found within the reported range of molecular weights (100-600 kDa) according to the experimental conditions used [21].

### 3.2. Physicochemical characterization of the films

#### Infrared spectroscopy

The infrared spectra of the non-crosslinked films (C0A, C25A, C50A, C75A and C100A) are shown in Fig. 2A. In the Col I film (C100A), five characteristic absorption bands were observed. The amide I band ( $1630 \text{ cm}^{-1}$ ) is originated from the C=O stretching vibrations coupled to N-H bending vibrations. The amide II ( $1546 \text{ cm}^{-1}$ ) arises due to N-H bending vibrations coupled to C-N stretching vibrations. The amide III ( $1246 \text{ cm}^{-1}$ ) represents the combination of peaks between the C-N stretching and N-H bending vibrations. The other two bands arise from the -OH ( $3445 \text{ cm}^{-1}$ ) and N-H ( $3300 \text{ cm}^{-1}$ ) stretching vibrations [26]. In addition, the bands of the commercial film were in approximately the same regions as the C100A film, denoting that they are the same substance.

In the spectrum of the CS film (C0A), the following characteristic absorption bands were observed. Between  $3500-3000 \text{ cm}^{-1}$  a wide signal is shown due to the stretching vibration of -OH ( $3452 \text{ cm}^{-1}$ ) and N-H ( $3311 \text{ cm}^{-1}$ ) groups, at  $1643 \text{ cm}^{-1}$  the stretching vibration of C=O group of the acetylated units appears, at  $1580 \text{ cm}^{-1}$  the bending vibration of -NH<sub>2</sub> group is evidenced and at  $1150 \text{ cm}^{-1}$  the stretching vibration of glycosidic bond (C-O-C) between the monomeric units of CS is seen [27].

The spectra of the Col I-CS films (C25A, C50A and C75A) illustrated similar characteristic peaks to the origin molecules (C0A and C100A). For example, the intensity of the amide I peak of Col I ( $1630\text{ cm}^{-1}$ ) decreases gradually as the proportion of CS increases. Besides, the intensity of the glycosidic bond of CS ( $1150\text{ cm}^{-1}$ ) decreases with the presence of Col I. These results suggest the existence of physical interactions (e.g., hydrogen bonds) between Col I and CS molecules, coinciding with Tangsadthakun *et al.* [28].

The absorption bands of the crosslinked films (C0B, C25B, C50B, C75B and C100B) (Fig. 2B), were presented in frequencies very similar to the non-crosslinked films, however, the intensity of these decreased due to crosslinking with EDC. The weakening of the bands intensities is because several carboxyl, amino and hydroxyl groups of Col I and CS participate in the crosslinking reaction to form amide and ester covalent bonds [29]. For example, the intensity of the amide I ( $1630\text{ cm}^{-1}$ ), amide II ( $1546\text{ cm}^{-1}$ ), amide III ( $1246\text{ cm}^{-1}$ ) and  $\delta_{-\text{NH}_2}$  ( $1580\text{ cm}^{-1}$ ) decreases with the crosslinking, suggesting that the  $-\text{NH}_2$  groups of Col I and CS are changed to N-H groups due to the formation of amide bonds between Col I molecules, or between Col I and CS molecules.

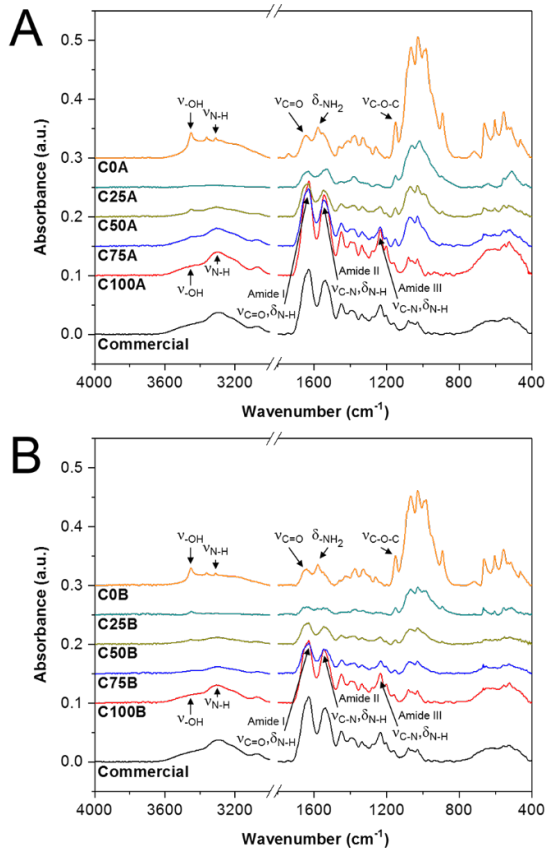


**Fig. 2.** FTIR spectra of the type I collagen-chitosan films A) non-crosslinked (C0A, C25A, C50A, C75A and C100A) and B) crosslinked with EDC (C0B, C25B, C50B, C75B and C100B); and spectrum of the commercial film.

## Water absorption

Hydrogels generally have a high water absorption capacity, which is favorable in tissue engineering since they can retain rich fluids in nutrients and cytokines that facilitate the stimulation of cells involved in tissue repair [30,31]. In Table 1, it is observed that the crosslinked films with EDC showed a lower absorption capacity, which could be attributed to the fact that 1) several hydrophilic groups present in Col I and CS (-NH<sub>2</sub> and -OH) are consumed in the crosslinking reaction according to infrared analysis and, 2) the pore size of the polymer networks decreases due to crosslinking, preventing that some water molecules are absorbed [32].

**Table 1.** Water absorption percentage by the type I collagen-chitosan films non-crosslinked and crosslinked with EDC; and by the commercial film (mean ± SD, n = 3).

Film	Water absorption (%)	
	Non-Crosslinking	Crosslinking
<b>C0</b>	122.9 ± 3.7	99.6 ± 3.3
<b>C25</b>	141.7 ± 4.0	132.2 ± 4.4
<b>C50</b>	175.8 ± 0.7	161.2 ± 8.9
<b>C75</b>	310.2 ± 26.6	259.0 ± 8.9
<b>C100</b>	842.8 ± 57.7	532.0 ± 30.0
<b>Commercial</b>	216.3 ± 3.6	

## Thermal analysis

In the DSC thermograms of the non-crosslinked films (Fig. 3A), an endothermic transition was observed in the temperatures range from 25 to 175 °C, which is due to dehydration by the loss of bonds between water molecules and polymer chains [33]. In the case of the DSC thermograms of the films crosslinked with EDC (Fig. 3B), these presented a thermal profile very similar to the non-crosslinked films, with the difference that the crosslinked films exhibited a displacement in temperature toward higher temperatures, indicating that this type of films requires a higher temperature to dehydrate. It should be mentioned that the dehydration process was confirmed with the TGA thermograms (Figs. 3A and B), because these showed low mass loss percentages in the endothermic transition (8-13%).

The values of temperature and enthalpy of dehydration ( $T_d$  and  $\Delta H_d$ , respectively) obtained from the DSC thermograms of the films are shown in Table 2. In this table, it is appreciated that the  $T_d$  and  $\Delta H_d$  of the films decreased with the presence of CS, however, the films crosslinked with EDC presented a higher temperature and enthalpy of dehydration. The increase in  $T_d$  and  $\Delta H_d$  could be due to the formation of new covalent bonds by the crosslinking that makes the polymeric structure more stable. In the case of the commercial film, the temperature and enthalpy were lower than some obtained films, indicating that the commercial film is dehydrated at a lower temperature and enthalpy.

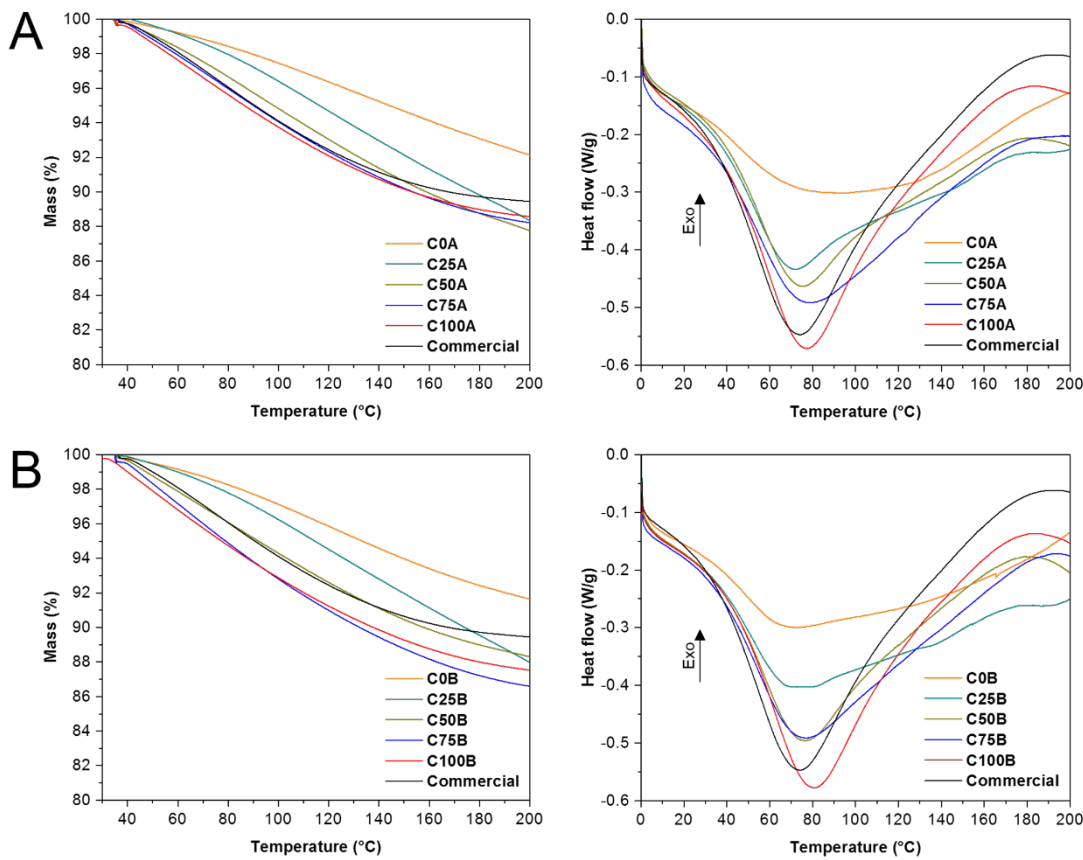


**Fig. 3.** TGA and DSC thermograms of the type I collagen-chitosan films A) non-crosslinked (C0A, C25A, C50A, C75A and C100A) and B) crosslinked with EDC (C0B, C25B, C50B, C75B and C100B); and thermograms of the commercial film. In the DSC analysis, the initial mass of the samples was the same because the heat flow is an extensive property.

**Table 2.** Temperature and enthalpy of dehydration of the type I collagen-chitosan films non-crosslinked and crosslinked with EDC; and of the commercial film.

Film	Td (°C)		ΔHd (J/g)	
	Non-Crosslinking	Crosslinking	Non-Crosslinking	Crosslinking
<b>C0</b>	68.5	72.1	158.2	173.4
<b>C25</b>	71.9	72.7	159.1	185.4
<b>C50</b>	74.9	76.6	215.2	229.8
<b>C75</b>	76.9	79.4	237.1	281.5
<b>C100</b>	77.3	80.6	278.6	288.1
<b>Commercial</b>	74.1		270.0	

## Mechanical test

The tested films were hydrated with PBS at 37 °C, in order to characterize them under similar conditions to those that will be in the body. The absorption capacity of hydrogels is intimately related to the mechanical and structural properties of these, therefore, their elastic behavior is highly dependent on the water amount they can absorb [34,35].

In Figs. 4A and B, it is observed that the films crosslinked with EDC presented, in general, a lower percentage of deformation at break, but a higher value of ultimate tensile strength (UTS) and Young's modulus (E). Since the mechanical response of hydrogels is strongly related to their water absorption capacity, it can be seen that a decrease in the water absorption percentage by the films implied an increase in their mechanical properties (UTS and E). This is due to the fact that 1) a crosslinked polymer network has a smaller space available to be occupied by the water molecules because the network pore size is decreased and, 2) by limiting the mobility of the polymer chains by the crosslinking, the elastic strength that opposes the water absorption is increased [32].

The ultimate tensile strength of the films (Fig. 4C) increased with the presence of CS, which could be attributed to the fact that this polymer has a lower water absorption percentage than Col I, according to the water absorption experiment. In Fig. 4D, it is appreciated that the Young's modulus of the CS films (C0) was low, however, this parameter improved when the Col I proportion was increased a little (C25) and, if this proportion was increasing even more (C50, C75 and C100), the elastic modulus was gradually decreasing. In these figures (Figs. 4C and D), it can also be seen that the crosslinked C25 film was the only obtained film that showed a similar value of ultimate tensile strength and Young's modulus to the commercial film.

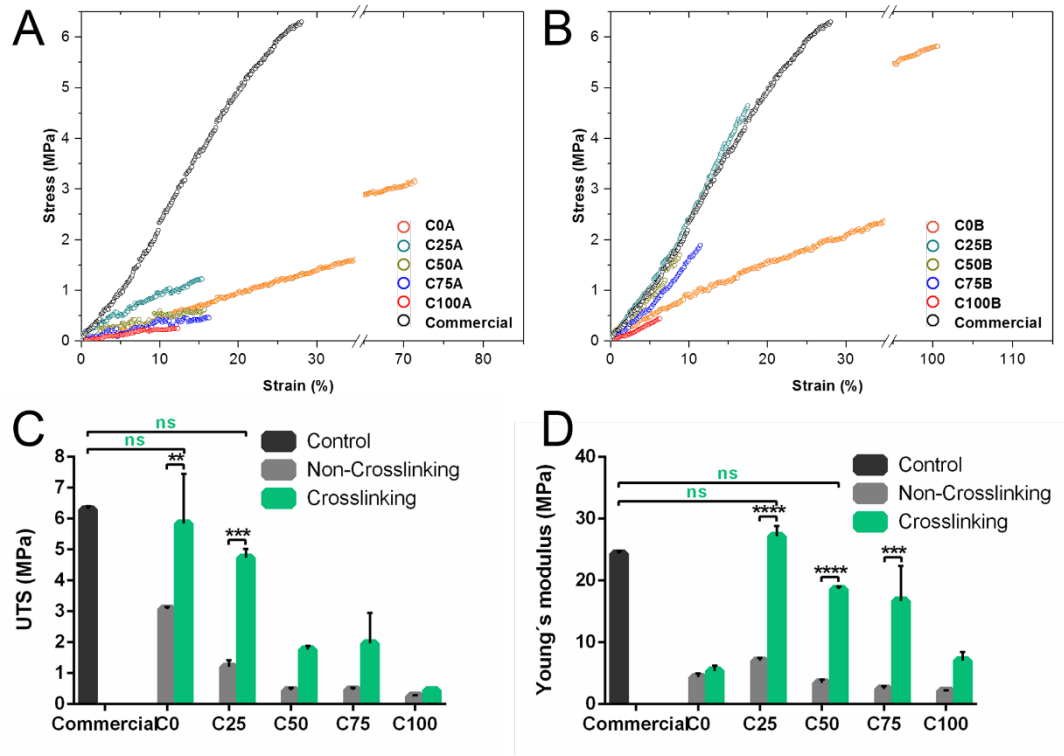


**Fig. 4.** Stress-strain curves of the type I collagen-chitosan films A) non-crosslinked (C0A, C25A, C50A, C75A and C100A) and B) crosslinked with EDC (C0B, C25B, C50B, C75B and C100B); and curve of the commercial film. C) Ultimate tensile strength (UTS) and D) Young's modulus (E) of the non-crosslinked and crosslinked films; and of the commercial film (ns indicates that there is no significant difference between the control and the obtained films and; \*\*p < 0.01, \*\*\*p < 0.001 and \*\*\*\*p < 0.0001 denote that there is a significant difference between the treatments).

### In vitro degradation

Scaffolds for guided bone regeneration have eventually to be degradable since they have to be replaced by new tissue [36]. Moreover, degradation byproducts do not have to be toxic nor have they to interfere with organ function [37]. The degradation of a film is important because this substrate has to separate the bone tissue from the gingival for a sufficient time ( $\geq 6$  months) in order to have an adequate bone repair [38].

The degradation of the films was evaluated by monitoring the residual mass of these after different incubation times in a lysozyme solution at a concentration of 112 000 U/mL, which corresponds to 1000 times the normal concentration of this enzyme in human plasma (112 U/mL) [39,40]. The reason why a high concentration of lysozyme was used was in order to accelerate the process of enzymatic digestion, and thus to know the short-term degradation behavior of the films. In Figs. 6A and B, it is observed that the films crosslinked with EDC were dissolved more slowly (degradation below 20%) than the non-crosslinked films (degradation up to 80%). The decrease in the degradation percentage could be due to the fact that the enzyme

has to cleave a higher amount of polymer chains due to the formation of new covalent bonds by the crosslinking.

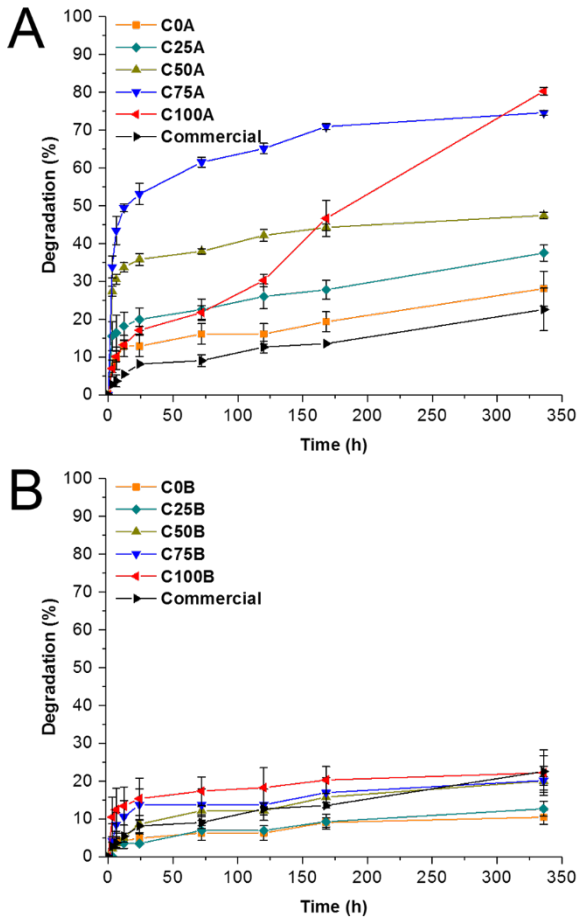


**Fig. 6.** Enzymatic degradation kinetics of the type I collagen-chitosan films A) non-crosslinked (C0A, C25A, C50A, C75A and C100A) and B) crosslinked with EDC (C0B, C25B, C50B, C75B and C100B); and kinetic of the commercial film using lysozyme.

## Morphology

The surface morphology of the films (Fig. 5A) was homogeneous, which could be attributed to the fact that Col I and CS are hydrophilic, allowing the miscibility of the polymer blends. Additionally, the roughness of the films was favored with the presence of Col I. According to Li *et al.* [41], the roughness of scaffolds surface is favorable for cell adhesion, which is discussed subsequently in the biological assays.

The films have to separate the bone tissue from the gingival, so it is important to observe their cross-section morphology to know if there can be any infiltration of unwanted cell tissues. The cross-section morphology of the films (Fig. 5B) was sufficiently compact and there was no presence of pores, except for the C100 film, in which very small pores were seen. Furthermore, the morphology of the films was not

affected by the crosslinking with EDC, because the surface and cross-section of the crosslinked films were very similar to the non-crosslinked films.

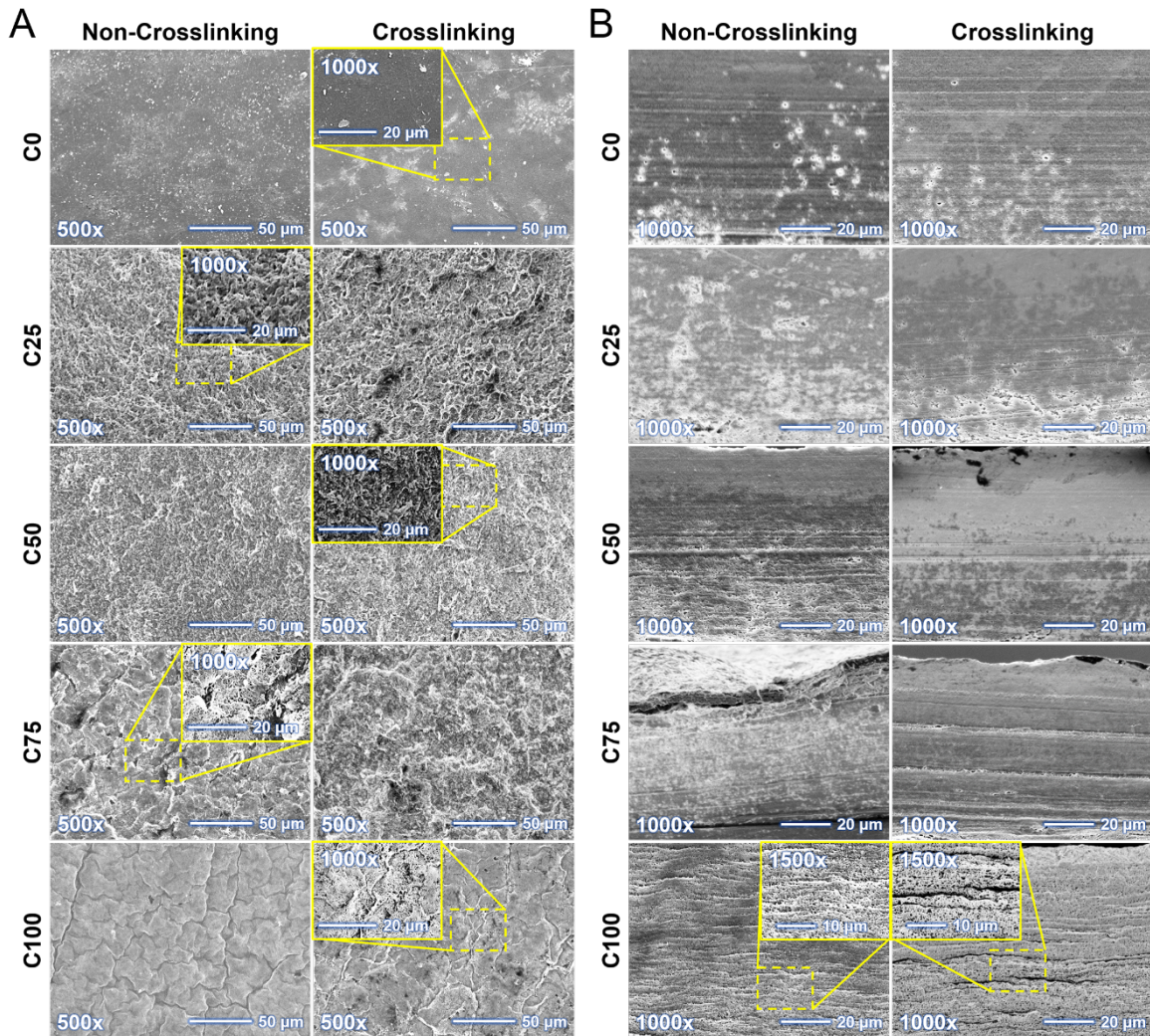


**Fig. 5.** A) Surface and B) cross-section morphology of the type I collagen-chitosan films non-crosslinked and crosslinked with EDC.

### 3.3. Biological characterization of the films

#### Cell adhesion

Since the properties of scaffolds (e.g., chemical composition, water absorption capacity, elastic modulus and roughness) can influence the cell response, understanding the cell-scaffold *in vitro* interaction is a first step to know the biocompatibility of the films that pretend to be used in guided tissue separation [42].

The differentiation and proliferation of cells are influenced by the adhesion and dissemination of these over scaffolds during the first stage of cell culture [43]. In this

way, the cell adhesion constitutes one of the previous requirements for evaluating the biocompatibility of the films.

The adhesion of human fetal osteoblasts (hFOB) onto the films was evaluated by the crystal violet method after 4 h of cell culture. The adhesion of hFOB cells (Fig. 7A) was favored with the presence of Col I and was not affected by the crosslinking with EDC. Although the chemical composition of the films could play an important role in cell adhesion, this response could also be related to the surface morphology of these, because when the surface was rougher, the adhesion was higher, coinciding with Li *et al.* [41]. In addition, the obtained films showed a higher cell adhesion percentage (75-125%) than the commercial film (60%).

### **Cell viability**

A good cell adhesion response indicates that the films do not biologically affect to the cells. In order to confirm the above, the viability of hFOB cells over the films was evaluated using the cell counting kit-8 (CCK-8), quantifying the optical density at 450 nm. The CCK-8 indicates the state of cell metabolism through the color change of tetrazolium salts by reducing to formazan when they are incubated with viable cells [24]. In this way, an increase in optical density indirectly indicates an increase in the viability or proliferation of cells as a result of cell metabolic activity.

In Figs. 7B and C, it is appreciated that the crosslinking with EDC did not affect to the cell viability because both types of films present a very similar viability profile and, besides, this cell response increases with respect to time. As well as the cell adhesion is related to the surface morphology of the films, the viability and adhesion of cells could also be related because an increase in adhesion implied an increase in viability, coinciding with Narayan [44].

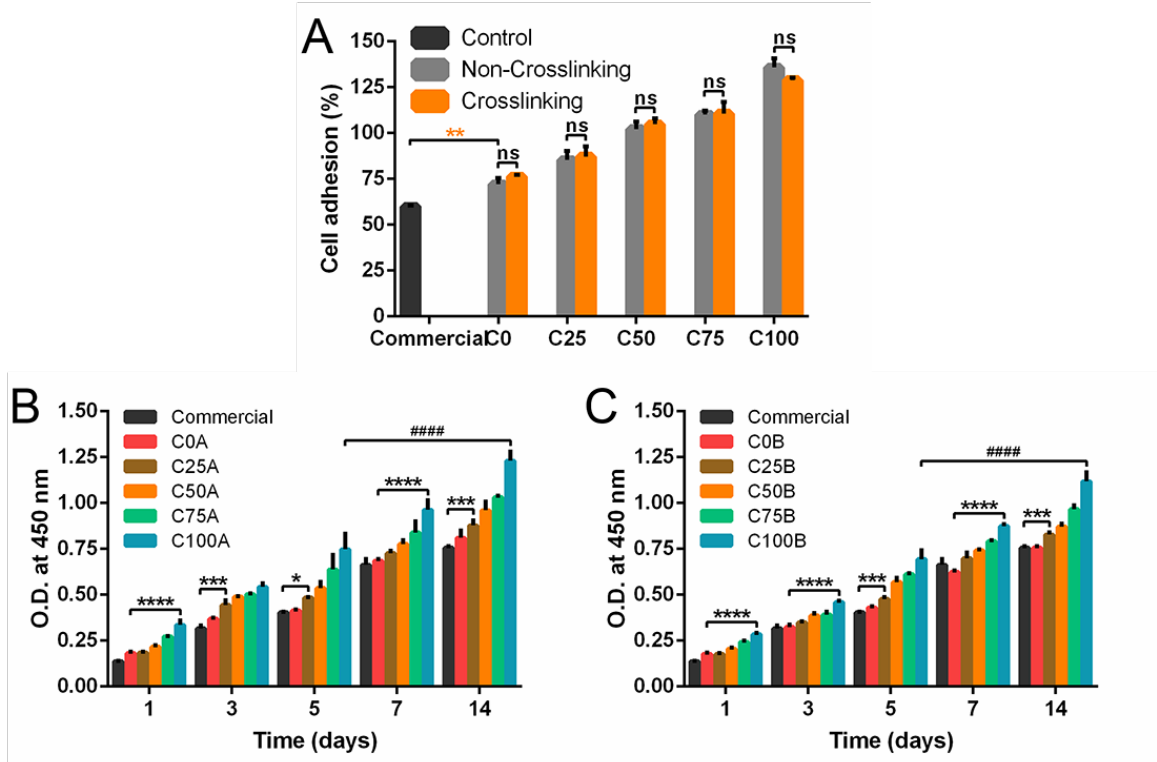


**Fig. 7.** A) Adhesion of the hFOB cells onto the type I collagen-chitosan films non-crosslinked and crosslinked with EDC; and onto the commercial film after 4 h of cell culture (\*\* p < 0.01 indicates that there is a significant difference between the control and the obtained films and; ns denotes that there is no significant difference between the treatments). Cell viability over the B) non-crosslinked (C0A, C25A, C50A, C75A and C100A) and C) crosslinked films (C0B, C25B, C50B, C75B and C100B); and viability over the commercial film at day 1, 3, 5, 7 and 14 of cell culture (\*p < 0.05, \*\*p < 0.001 and \*\*\*p < 0.0001 denote that there is a significant difference between the films and; #####p < 0.0001 indicates that there is significant difference between the films at different cell culture time).

## Cell morphology

According to Narayan [44], cell morphology provides evidence of its biocompatibility degree with the scaffold. In this way, an indicator that a cell interacts well with the scaffold is the speed at which it extends onto the surface and loses the spherical shape that it assumed while it was in the cell suspension.

In Fig. 8, it is observed that the hFOB cells were able to colonize and spread over the surface of the films crosslinked with EDC suggesting a good biocompatibility between them. In the crosslinked C0 film (Fig. 8A), the cells were isolated or in small dispersed groups and some cells presented a rounded cytoplasm. This type of cell morphology indicates a poor adherence to the films, which could be due to the fact that the surface of this film is less rough than the rest. In the other crosslinked films (Figs. 8B-E), the cells exhibited a polyhedral morphology that is characteristic of the hFOB cells. Additionally, some adhesion points of the cells (filopodia) in contact with the surface of the films were appreciated, which could be interpreted as a biological response to the morphology of the films. This response is important because it provides an

adequate environment for cell adhesion to take place and afterward cells can proliferate. Moreover, some cells synthesized extracellular matrix (ECM). The synthesis of ECM by cells is one more indicative of their adhesion to the films, because it is known that cells depend on their adhesion to a substrate for their growth, proliferation and synthesis of ECM. Therefore, these results suggest that the chemical composition and surface morphology of the films have a great influence on adhesion, viability and morphology of cells.

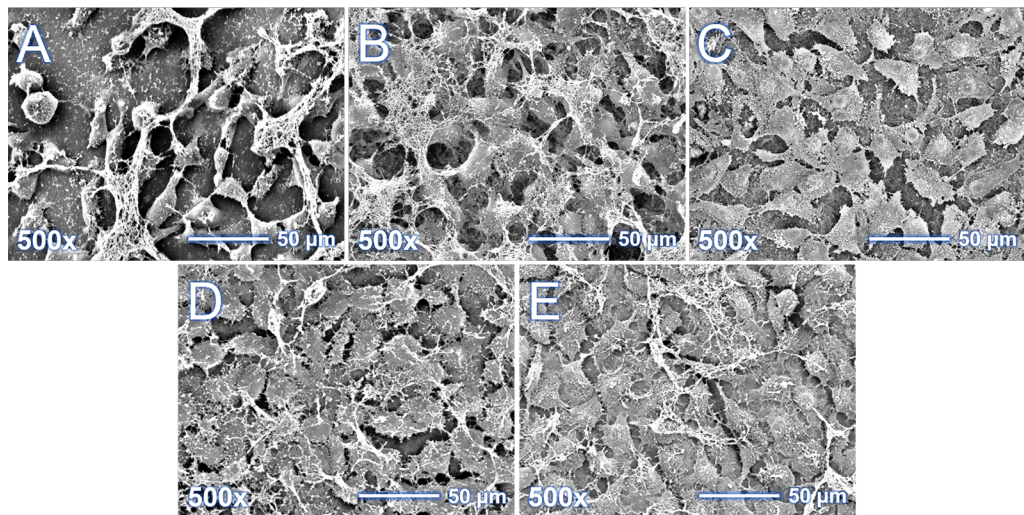


**Fig. 8.** Morphology of the hFOB cells onto the A) C0, B) C25, C) C50, D) C75, E) C100 films crosslinked with EDC at 24 h of cell culture.

#### 4. Conclusions

The obtained type I collagen had a high purity degree, indicating that the methodology used is adequate to obtain the protein. The method used for the extraction of chitin and its conversion to chitosan, allowed obtaining products with a high degree of deacetylation (96.5%) and an appropriate molecular weight (145.2 kDa) for the preparation of the films. The production of type I collagen-chitosan films with the solvent evaporation technique is a good alternative in guided bone regeneration since the films present a rough surface that is adequate for cell adhesion and a compact cross-section to prevent some infiltration of unwanted cell tissues. According to the physicochemical and biological characterization of the films, the chemical crosslinking with EDC improves the resistance to dehydration, tensile strength and enzymatic digestion; and is not cytotoxic. Therefore, the results obtained in this work demonstrated that the type I collagen-chitosan films crosslinked with EDC are a better option for their use in guided bone regeneration, specifically, the C25 crosslinked films due to their mechanical properties.

## Acknowledgments

To CONACyT for the scholarship granted with No. 418423 and to DGAPA-UNAM for the financial support provided through the PAPIIT IT100114, IT100117 and IT203618 projects. We thank to Nayeli Rodríguez Fuentes, Karla Eriseth Reyes Morales, José Ocotlán Flores Flores, Armando Zepeda Rodríguez, Francisco Pasos Nájera and Carlos Flores Morales for their technical assistance.

## References

- [1] D. González Fernández, G. Olmos Sanz, C. López Niñoles, D. Calzavara Mantovani, G. Cabello Domínguez, Membranas no reabsorbibles en implantología. Razonamiento actual para su uso e indicaciones, Periodoncia y Osteointegración. 15 (2005) 295–308. <https://www.sepa.es/images/stories/SEPA/PDF/15-5.pdf>.
- [2] D. González Padilla, A. García-Perla García, J.L. Gutiérrez Pérez, D. Torres Lagares, G. Castillo Dali, M. Salido Peracaula, J. Vilches Troya, J.I. Vilches Pérez, A. Terriza Fernández, Á. Barranco Quero, F. Yubero Valencia, A. Díaz Cuenca, A. Rodríguez González-Elipe, Membrana reabsorbible para regeneración ósea guiada, ES 2497240 B1, 2014. <http://hdl.handle.net/10261/123964>.
- [3] N. Shanmugasundaram, P. Ravichandran, P. Neelakanta Reddy, N. Ramamurty, S. Pal, K. Panduranga Rao, Collagen-chitosan polymeric scaffolds for the in vitro culture of human epidermoid carcinoma cells, Biomaterials. 22 (2001) 1943–1951. doi:10.1016/S0142-9612(00)00220-9.
- [4] S.P. Zhong, Y.Z. Zhang, C.T. Lim, Tissue scaffolds for skin wound healing and dermal reconstruction, Wiley Interdiscip. Rev. Nanomedicine Nanobiotechnology. 2 (2010) 510–525. doi:10.1002/wnan.100.
- [5] D.L. Nelson, M.M. Cox, Lehninger principles of biochemistry, 6th ed., W. H. Freeman, New York, 2013.
- [6] B. Alberts, A. Johnson, J. Lewis, D. Morgan, M. Raff, K. Roberts, P. Walter, J. Wilson, T. Hunt, Molecular biology of the cell, 6th ed., Garland Science/Taylor & Francis, New York, 2015.
- [7] J.A.M. Ramshaw, Y.Y. Peng, V. Glattauer, J.A. Werkmeister, Collagens as biomaterials, J. Mater. Sci. Mater. Med. 20 (2009) 3–8. doi:10.1007/s10856-008-3415-4.
- [8] P. Fratzl, ed., Collagen, Springer, Boston, MA, 2008. doi:10.1007/978-0-387-73906-9.
- [9] C. Han, L. Zhang, J. Sun, H. Shi, J. Zhou, C. Gao, Application of collagen-chitosan/fibrin glue asymmetric scaffolds in skin tissue engineering, J. Zhejiang

Univ. Sci. B. 11 (2010) 524–530. doi:10.1631/jzus.B0900400.

- [10] C. Lárez Velásquez, Algunos usos del quitosano en sistemas acuosos, Rev. Iberoam. Polímeros. 4 (2003) 91–109. <http://www.ehu.eus/reviberpol/pdf/ABR03/Cristobal2003.pdf>.
- [11] K.-Y. Chen, W.-J. Liao, S.-M. Kuo, F.-J. Tsai, Y.-S. Chen, C.-Y. Huang, C.-H. Yao, Asymmetric chitosan membrane containing collagen I nanospheres for skin tissue engineering, Biomacromolecules. 10 (2009) 1642–1649. doi:10.1021/bm900238b.
- [12] K. Madhavan, D. Belchenko, A. Motta, W. Tan, Evaluation of composition and crosslinking effects on collagen-based composite constructs, Acta Biomater. 6 (2010) 1413–1422. doi:10.1016/j.actbio.2009.09.028.
- [13] J. Hua, Z. Li, W. Xia, N. Yang, J. Gong, J. Zhang, C. Qiao, Preparation and properties of EDC/NHS mediated crosslinking poly (gamma-glutamic acid)/epsilon-polylysine hydrogels, Mater. Sci. Eng. C. 61 (2016) 879–892. doi:10.1016/j.msec.2016.01.001.
- [14] W. Li, Y. Long, Y. Liu, K. Long, S. Liu, Z. Wang, Y. Wang, L. Ren, Fabrication and characterization of chitosan–collagen crosslinked membranes for corneal tissue engineering, J. Biomater. Sci. Polym. Ed. 25 (2014) 1962–1972. doi:10.1080/09205063.2014.965996.
- [15] X.H. Wang, D.P. Li, W.J. Wang, Q.L. Feng, F.Z. Cui, Y.X. Xu, X.H. Song, M. van der Werf, Crosslinked collagen/chitosan matrix for artificial livers, Biomaterials. 24 (2003) 3213–3220. doi:10.1016/S0142-9612(03)00170-4.
- [16] E.J. Miller, R. Kent Rhodes, Preparation and characterization of the different types of collagen, in: L.W. Cunningham, D.W. Frederiksen (Eds.), Methods Enzymol., Academic Press, 1982: pp. 33–64. doi:10.1016/0076-6879(82)82059-4.
- [17] J.F. Robyt, B.J. White, Biochemical techniques: Theory and practice, Waveland Press, Illinois, 1987.
- [18] J.F. Woessner, The determination of hydroxyproline in tissue and protein samples containing small proportions of this imino acid, Arch. Biochem. Biophys. 93 (1961) 440–447. doi:10.1016/0003-9861(61)90291-0.
- [19] S.P. Miranda Castro, A.V. Lara Sagahón, Proceso para la extracción de quitina a partir de exoesqueletos de crustáceos y su conversión a quitosán, MX 293022 B, 2000.  
<http://sigia.impi.gob.mx/newSIGA/content/common/ficha.jsf?idFicha=4910106>.

- [20] E.S. de Alvarenga, Characterization and properties of chitosan, in: M. Elnashar (Ed.), *Biotechnol. Biopolym.*, InTech, 2011: pp. 91–108. doi:10.5772/17020.
- [21] M.R. Kasaai, Calculation of Mark-Houwink-Sakurada (MHS) equation viscometric constants for chitosan in any solvent-temperature system using experimental reported viscometric constants data, *Carbohydr. Polym.* 68 (2007) 477–488. doi:10.1016/j.carbpol.2006.11.006.
- [22] N. Rivera, S.E. Romero, Á. Menchaca, A. Zepeda, L.E. García, G. Salas, L. Romero, F. Malagón, Blackwater fever like in murine malaria, *Parasitol. Res.* 112 (2013) 1021–1029. doi:10.1007/s00436-012-3224-z.
- [23] A.A. Altamirano Valencia, N. Vargas Becerril, F.C. Vázquez Vázquez, T. Vargas Koudriavtsev, J.J. Montesinos Montesinos, E. Alfaro Mayorga, M.A. Álvarez Pérez, Biocompatibility of nanofibrous scaffolds with different concentrations of PLA/hydroxyapatite, *Odontos - Int. J. Dent. Sci.* 18 (2016) 39–50. doi:10.15517/ijds.v0i0.25987.
- [24] Sigma-Aldrich, Cell Counting Kit - 8, n.d. <https://www.sigmaaldrich.com/content/dam/sigma-aldrich/docs/Sigma/Datasheet/6/96992dat.pdf> (accessed October 15, 2018).
- [25] S. Nalinanon, S. Benjakul, W. Visessanguan, H. Kishimura, Use of pepsin for collagen extraction from the skin of bigeye snapper (*Priacanthus tayenus*), *Food Chem.* 104 (2007) 593–601. doi:10.1016/j.foodchem.2006.12.035.
- [26] C. Ungureanu, D. Ioniță, E. Berteau, L. Tcacenco, A. Zuav, I. Demetrescu, Improving natural biopolymeric membranes based on chitosan and collagen for biomedical applications introducing silver, *J. Braz. Chem. Soc.* 26 (2015) 458–465. doi:10.5935/0103-5053.20150298.
- [27] N.E. Suyatma, A. Copinet, E. Legin-Copinet, F. Fricoteaux, V. Coma, Different PLA grafting techniques on chitosan, *J. Polym. Environ.* 19 (2011) 166–171. doi:10.1007/s10924-010-0269-x.
- [28] C. Tangsadthakun, S. Kanokpanont, N. Sanchavanakit, T. Banaprasert, S. Damrongsakkul, Properties of collagen/chitosan scaffolds for skin tissue engineering, *J. Met. Mater. Miner.* 16 (2006) 37–44. <http://ojs.materialsconnex.com/index.php/jmmm/article/view/250/277>.
- [29] F. Zhang, C. He, L. Cao, W. Feng, H. Wang, X. Mo, J. Wang, Fabrication of gelatin-hyaluronic acid hybrid scaffolds with tunable porous structures for soft tissue engineering, *Int. J. Biol. Macromol.* 48 (2011) 474–481. doi:10.1016/j.ijbiomac.2011.01.012.
- [30] V. Shabafrooz, M. Mozafari, G.A. Köhler, S. Assefa, D. Vashaee, L. Tayebi, The effect of hyaluronic acid on biofunctionality of gelatin-collagen intestine tissue

engineering scaffolds, *J. Biomed. Mater. Res. Part A*. 102 (2014) 3130–3139. doi:10.1002/jbm.a.34984.

- [31] T. Maver, U. Maver, K.S. Kleinschek, I.M. Raščan, D.M. Smrke, Advanced therapies of skin injuries, *Wien. Klin. Wochenschr.* 127 (2015) 187–198. doi:10.1007/s00508-015-0859-7.
- [32] Y. Liu, N.E. Vrana, P.A. Cahill, G.B. McGuinness, Physically crosslinked composite hydrogels of PVA with natural macromolecules: Structure, mechanical properties, and endothelial cell compatibility, *J. Biomed. Mater. Res. Part B Appl. Biomater.* 90B (2009) 492–502. doi:10.1002/jbm.b.31310.
- [33] P. Jithendra, A.M. Rajam, T. Kalaivani, A.B. Mandal, C. Rose, Preparation and characterization of aloe vera blended collagen-chitosan composite scaffold for tissue engineering applications, *ACS Appl. Mater. Interfaces.* 5 (2013) 7291–7298. doi:10.1021/am401637c.
- [34] K.S. Anseth, C.N. Bowman, L. Brannon-Peppas, Mechanical properties of hydrogels and their experimental determination, *Biomaterials.* 17 (1996) 1647–1657. doi:10.1016/0142-9612(96)87644-7.
- [35] O. Jeon, S.J. Song, K.-J. Lee, M.H. Park, S.-H. Lee, S.K. Hahn, S. Kim, B.-S. Kim, Mechanical properties and degradation behaviors of hyaluronic acid hydrogels cross-linked at various cross-linking densities, *Carbohydr. Polym.* 70 (2007) 251–257. doi:10.1016/j.carbpol.2007.04.002.
- [36] M.N. Collins, C. Birkinshaw, Hyaluronic acid based scaffolds for tissue engineering—A review, *Carbohydr. Polym.* 92 (2013) 1262–1279. doi:10.1016/j.carbpol.2012.10.028.
- [37] F.J. O'Brien, Biomaterials & scaffolds for tissue engineering, *Mater. Today.* 14 (2011) 88–95. doi:10.1016/S1369-7021(11)70058-X.
- [38] J. Wang, L. Wang, Z. Zhou, H. Lai, P. Xu, L. Liao, J. Wei, Biodegradable polymer membranes applied in guided bone/tissue regeneration: A review, *Polymers (Basel).* 8 (2016) 115. doi:10.3390/polym8040115.
- [39] J. Brouwer, T. van Leeuwen-Herberts, M.O. de Ruit, Determination of lysozyme in serum, urine, cerebrospinal fluid and feces by enzyme immunoassay, *Clin. Chim. Acta.* 142 (1984) 21–30. doi:10.1016/0009-8981(84)90097-4.
- [40] B. Porstmann, K. Jung, H. Schmechta, U. Evers, M. Pergande, T. Porstmann, H.-J. Kramm, H. Krause, Measurement of lysozyme in human body fluids: Comparison of various enzyme immunoassay techniques and their diagnostic application, *Clin. Biochem.* 22 (1989) 349–355. doi:10.1016/S0009-9120(89)80031-1.

- [41] W. Li, R. Guo, Y. Lan, Y. Zhang, W. Xue, Y. Zhang, Preparation and properties of cellulose nanocrystals reinforced collagen composite films, *J. Biomed. Mater. Res. Part A*. 102 (2014) 1131–1139. doi:10.1002/jbm.a.34792.
- [42] Z. He, L. Xiong, Evaluation of physical and biological properties of polyvinyl alcohol/chitosan blend films, *J. Macromol. Sci. Part B*. 51 (2012) 1705–1714. doi:10.1080/00222348.2012.657584.
- [43] H.S. Mansur, E. de S. Costa, A.A.P. Mansur, E.F. Barbosa-Stancioli, Cytocompatibility evaluation in cell-culture systems of chemically crosslinked chitosan/PVA hydrogels, *Mater. Sci. Eng. C*. 29 (2009) 1574–1583. doi:10.1016/j.msec.2008.12.012.
- [44] R. Narayan, ed., *Biomedical Materials*, Springer, Boston, MA, 2009. doi:10.1007/978-0-387-84872-3.